Current Biology 20, 2003–2009, November 23, 2010 ©2010 Elsevier Ltd All rights reserved DOI 10.1016/j.cub.2010.09.061

Report

Electrostatic Cell-Surface Repulsion Initiates Lumen Formation in Developing Blood Vessels

Boris Strilić,[1,2] Jan Eglinger,[1] Michael Krieg,[3] Martin Zeeb,[1] Jennifer Axnick,[1] Pavel Babál,[4] Daniel J. Müller,[3,5] and Eckhard Lammert[1,*]

[1]Institute of Metabolic Physiology, Heinrich-Heine-University of Düsseldorf, D-40225 Düsseldorf, Germany

[2]Department of Pharmacology, Max Planck Institute for Heart and Lung Research, W.G. Kerckhoff-Institute, D-61231 Bad Nauheim, Germany

[3]Biotechnology Center, University of Technology Dresden, D-01307 Dresden, Germany

[4]Department of Pathology, Comenius University, SK-81108 Bratislava, Slovakia

[5]Biosystems Science and Engineering, Eidgenössische Technische Hochschule, Zürich, CH-4058 Basel, Switzerland

Summary

Blood vessels function in the uptake, transport, and delivery of gases and nutrients within the body. A key question is how the central lumen of blood vessels develops within a cord of vascular endothelial cells. Here, we demonstrate that sialic acids of apical glycoproteins localize to apposing endothelial cell surfaces and generate repelling electrostatic fields within an endothelial cell cord. Both in vitro and in vivo experiments show that the negative charge of sialic acids is required for the separation of endothelial cell surfaces and subsequent lumen formation. We also demonstrate that sulfate residues can substitute for sialic acids during lumen initiation. These results therefore reveal a key step in the creation of blood vessels, the most abundant conduits in the vertebrate body. Because negatively charged mucins and proteoglycans are often found on luminal cell surfaces, it is possible that electrostatic repulsion is a general principle also used to initiate lumen formation in other organs.

Results and Discussion

Mucins and proteoglycans are found on the luminal side of tubular organs in vertebrates, for example the gut, pancreas, salivary gland, lung, kidney, and blood vessels [1–5]. In addition, these glycoproteins are found on the apical surfaces of invertebrate tubular organs, such as the retina, tracheae, and wing imaginal discs of *Drosophila melanogaster*; the excretory cells of *Caenorhabditis elegans*; or the midgut of the *Anopheles* mosquito [6–10]. Interestingly, epithelial and endothelial cells express one such mucin, the CD34 sialomucin Podocalyxin/gp135 (PODXL), at the cell-cell contact at the onset of lumen formation (Figure 1) [1, 11, 12]. As with many mucins, the CD34 sialomucin extracellular domain is decorated with oligosaccharides containing a large number of negatively charged sialic acids [13]. Because the vascular lumen has previously been shown to develop through separation of adjacent endothelial cell (EC) surfaces during both vasculogenesis and angiogenesis [1, 14–16], we examined whether sialic acids of apical cell-surface proteins contribute an electrostatic repulsion to initiate this process. We first analyzed the developing mouse aorta (Figure 1), where a temporally and spatially defined transition from a nonlumenized EC cord to a lumenized tube takes place [1]. We find that sialic acids, detected with the *Tritrichomonas mobilensis* lectin [17], appear at the cell-cell contact (Figures 1A and 1B) and colocalize with the apical marker PODXL at the cell-cell contact and luminal cell surfaces (data not shown). These data suggest that the sialic acids on apical cell-surface proteins are positioned to separate apposing EC surfaces from each other to initiate blood vessel lumen formation in the developing mouse embryo.

It was previously shown that sialic acids can be removed from CD34 sialomucins by the enzymatic activity of neuraminidases, also known as sialidases [18]. To test whether sialic acids are required for vascular lumen formation in vivo, we injected neuraminidase into the mesenchyme of mouse embryos at the onset of aortic lumen formation and allowed these embryos to develop in whole-embryo culture (WEC) (Figure 1) [1]. We found that the injection of neuraminidase significantly reduced the presence of sialic acids at the endothelial cell-cell contact (compare Figures 1A and 1B with Figures 1E and 1F). More importantly, these neuraminidase-treated embryos developed fewer lumenized aortae when compared with controls (compare Figures 1C and 1D with Figures 1G and 1H). The only lumenized dorsal aortae to develop were observed cranially and caudally, far away from the injection sites (data not shown).

Because sialic acids strongly contribute to the negative charge of apical cell-surface proteins, we asked whether the negative charges of the apposing EC surfaces were required for vascular lumen formation. More precisely, we first asked whether reintroduction of negative charge to the neuraminidase-treated ECs could restore lumen formation (Figure S1, available online). To this end, we injected dextran sulfate into mouse embryos, a negatively charged molecule that has been shown to bind to the apical cell surfaces of injured ECs in vivo [19, 20]. In our developing mouse aorta model, we showed that dextran sulfate binds to the neuraminidase-treated apical cell surface of ECs (Figures S1I–S1K) and that it restores aortic lumen formation despite the absence of sialic acids (Figures S1I–S1M). In contrast, uncharged dextran does not rescue aortic lumen formation (Figures S1A–S1H). Importantly, neither treatment affected the EC viability or the expression of PODXL, moesin, and F-actin at the apical cell surface (Figure 1, Figure S1, and data not shown).

Second, we asked whether neutralization of the negative charge could inhibit lumen formation. We therefore injected into mouse embryos the cationic protamine sulfate, which was shown to neutralize the negative charge of sialic acids [21]. This injection significantly reduced the sialic acid staining, showing that protamine sulfate effectively masked the sialic acids (compare Figures 1A and 1B with Figures 1I and 1J). More importantly, vascular lumen formation was reduced when compared to control (compare Figures 1C and 1D with Figures 1K and 1L). Taken together, these data strongly suggest that sialic acids and their negative charge are required

*Correspondence: lammert@uni-duesseldorf.de

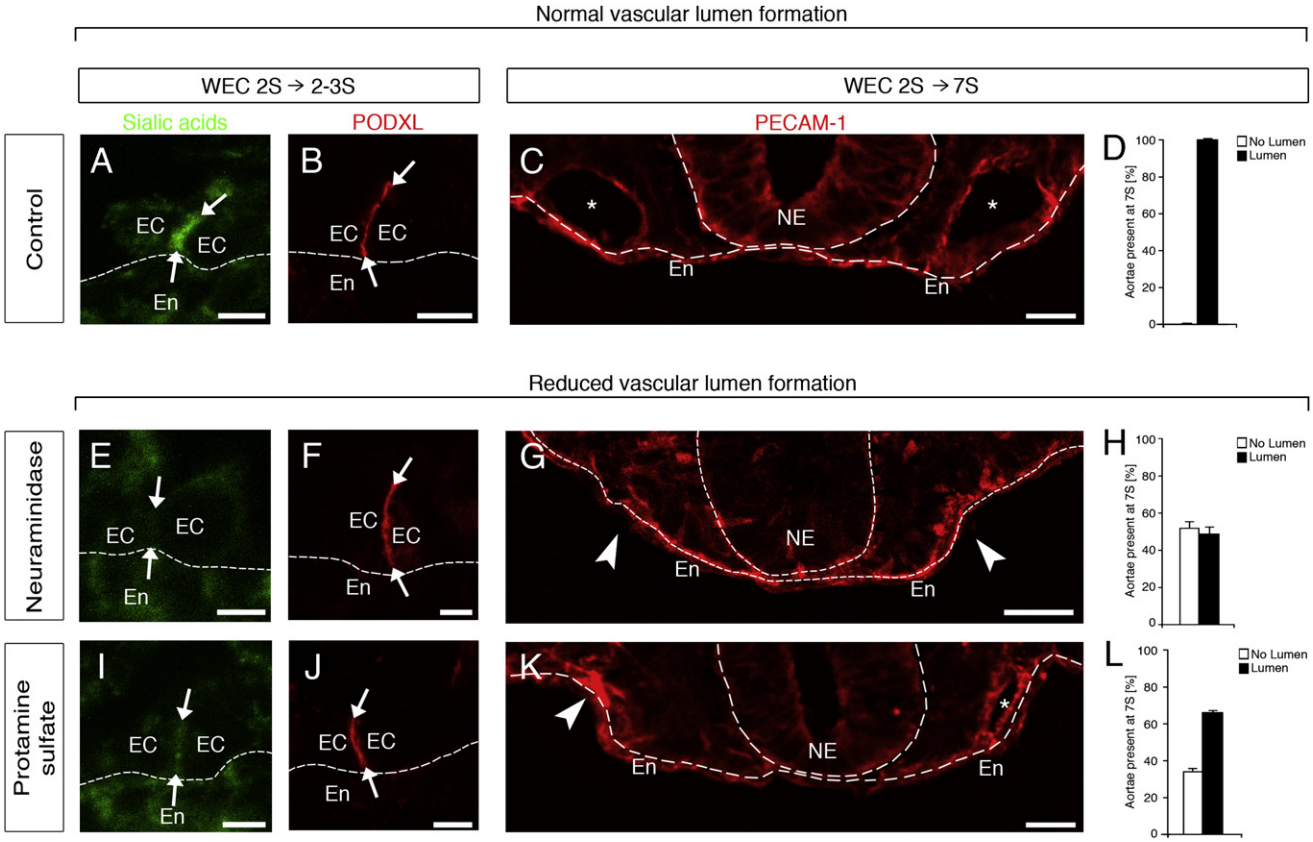

Figure 1. Removal of Sialic Acids or Neutralization of the Negative Charge Inhibits Blood Vessel Lumen Formation

Confocal images of transverse sections through the developing mouse dorsal aortae and quantification of blood vessel lumen formation.

(A–D) Effects of poly-DL-alanine (control), (E–H) neuraminidase, and (I–L) protamine sulfate on the localization of sialic acids and PODXL at the endothelial cell-cell contact and on aortic lumen formation (asterisks).

(A, B, E, F, I, and J) Confocal images showing (A, E, and I) sialic acids or (B, F, and J) PODXL on transverse sections through dorsal aortae after WEC of mouse embryos from the 2S to 2–3S stage for 30 min. Arrows point to the endothelial cell-cell contact.

(C, G, and K) Confocal images showing PECAM-1 endothelial staining on transverse sections through dorsal aortae after WEC from the 2S to 7S stage for 5–7 hr after the treatment indicated on the left. Arrowheads point to nonlumenized dorsal aortae, whereas asterisks mark the vascular lumen.

The following abbreviations are used: EC, endothelial cell; En, endoderm; NE, neuroepithelium. Scale bars represent 5 μm (A, B, E, F, I, and J) and 20 μm (C, G, and K).

(D, H, and L) Quantification of EC cords ("No Lumen," white bar) and vascular tubes ("Lumen," black bar) after WEC from the 2S to 7S stage following the treatment indicated on the left. $n \geq 100$ aortic sections of $n \geq 3$ embryos per condition. All values are means ± SD.

on the apical EC surface for initiating a blood vessel lumen in the developing mouse embryo.

We next investigated whether sialic acids and their negative charge reduce adhesion of apposing EC surfaces (Figure 2). To this end, we established a bead rolling assay (BRA) (Figure 2A) in which human umbilical vein endothelial cells (HUVECs) expressing sialic acids at their apical EC surface were grown on collagen I-coated beads and cell culture dishes (Figures 2A and 2B and data not shown). The EC-covered beads were then transferred to the tilted EC monolayer to determine their rolling distance over time (Figure 2A). This distance is an inverse measure for the adhesion of the apposing EC surfaces because cell-cell adhesion is supposed to counteract gravity and thus inhibits the rolling of the beads. Indeed, the rolling distance of the beads increased with the steepness of the cell culture dish (Figure 2J). Using the BRA, we found that neuraminidase-treated ECs had fewer sialic acids on their apical EC surface (compare Figures 2A and 2B with Figures 2D and 2E, and see Figure 2K) and rolled over a significantly shorter distance compared to control (12% ± 4%, $p < 0.01$) (compare Figure 2C with Figure 2F and see Figure 2L and Movie S1). Moreover, addition of dextran sulfate, but not dextran, partially rescued the bead rolling, indicating that the negative charge is required for reducing cell-cell adhesion (Figure S2 and Movie S2). Furthermore, treatment with protamine sulfate masked the sialic acids on apical EC surfaces (compare Figures 2A and 2B with Figures 2G and 2H, and see Figure 2K), and the beads rolled over a shorter distance compared to control (28% ± 5%, $p < 0.001$) (compare Figure 2C with Figure 2I and see Figure 2L and Movie S1). Incubation of washed HUVECs for 30 min and for 24 hr reversed the effects of protamine sulfate and neuraminidase, respectively (Figure 2L). These results demonstrate that the negative charge of sialic acids is required for reducing the adhesion between apposing EC surfaces.

Next, we quantified the adhesion strength between apposing ECs by using single-cell force spectroscopy (SCFS) (Figure 3), which is based on atomic force microscopy (AFM) [22, 23]. Here, the EC surfaces were brought into contact with each other and, after a dwell time of 1, 10, or 20 s, we recorded the

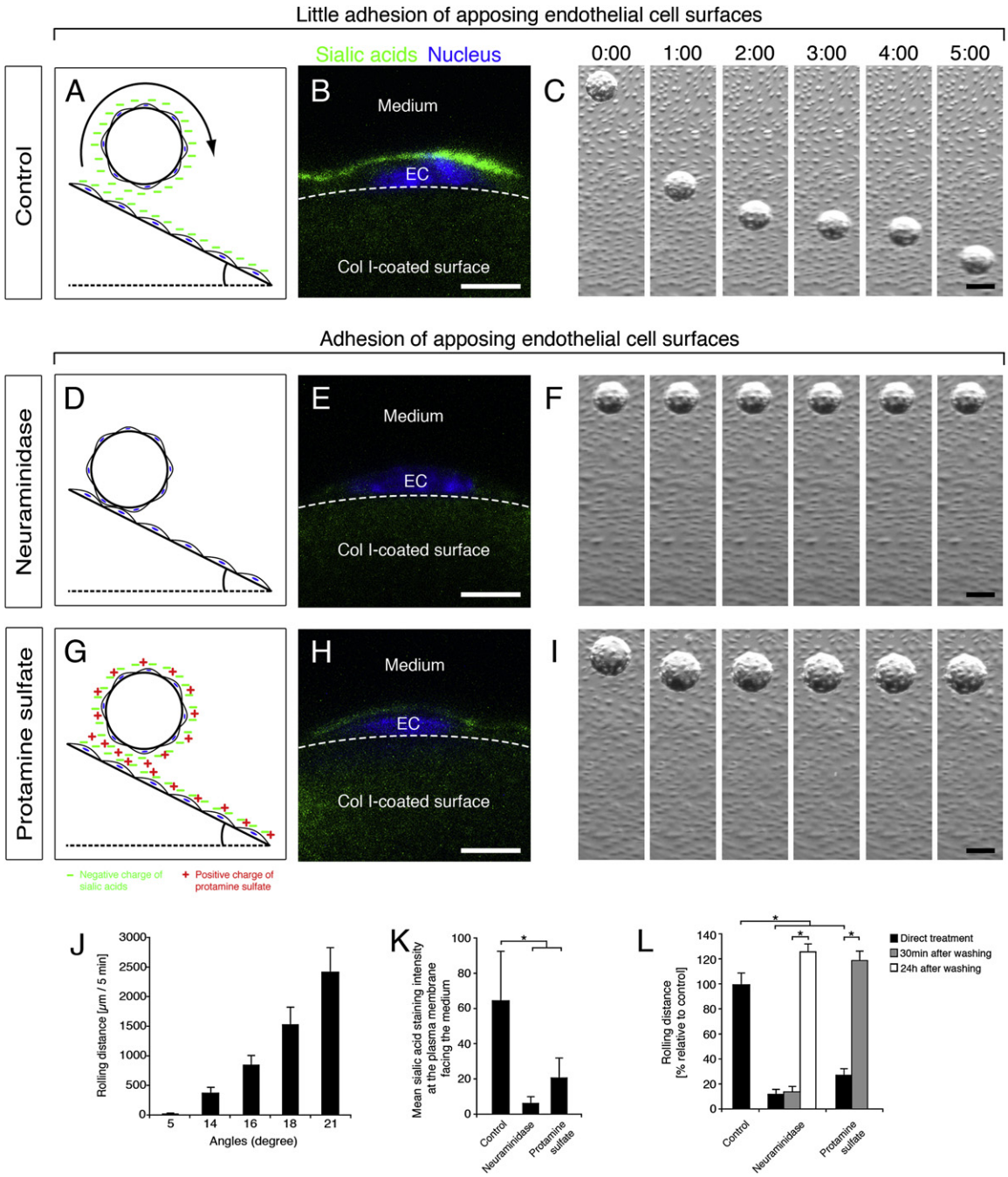

Figure 2. Sialic Acids and Negative Cell-Surface Charges Are Required for Deadhesion of Apposing Endothelial Cell Surfaces

(A, D, and G) Schematic diagram of a BRA experiment under (A) control conditions and after treatment with (D) neuraminidase or (G) protamine sulfate. The negative charges of sialic acids are shown in green (−) and the positive charges of protamine sulfate are shown in red (+). A black arrow indicates the rolling of the HUVEC-coated beads on the tilted HUVEC monolayer.

(B, E, and H) Confocal images of transverse sections through ECs grown on collagen I-coated beads and stained for sialic acids after the treatment indicated on the left.

(C, F, and I) Bright-field images of movies showing EC-coated beads rolling on a tilted EC monolayer. Time is indicated in min:s. See also Movie S1. Scale bars represent 5 μm (B, E, and H) and 100 μm (C, F, and I).

(J) Quantification of the rolling distance in relation to the steepness of the monolayer. $n \geq 90$ beads per angle (degree). All values are means ± SD.

(K) Quantification of the fluorescence intensity of sialic acid staining on the surface of ECs grown on collagen I-coated beads after the treatment indicated below. $n \geq 10$ beads per treatment. *$p < 0.05$. All values are means ± SD.

(L) Quantification of the rolling distance of EC-coated beads on a tilted EC monolayer directly after treatment (black bars), 30 min after washing (gray bars), or 24 hr after washing (white bar). $n \geq 300$ beads per treatment from $n \geq 3$ independent experiments. *$p < 0.05$. All values are means ± SEM.

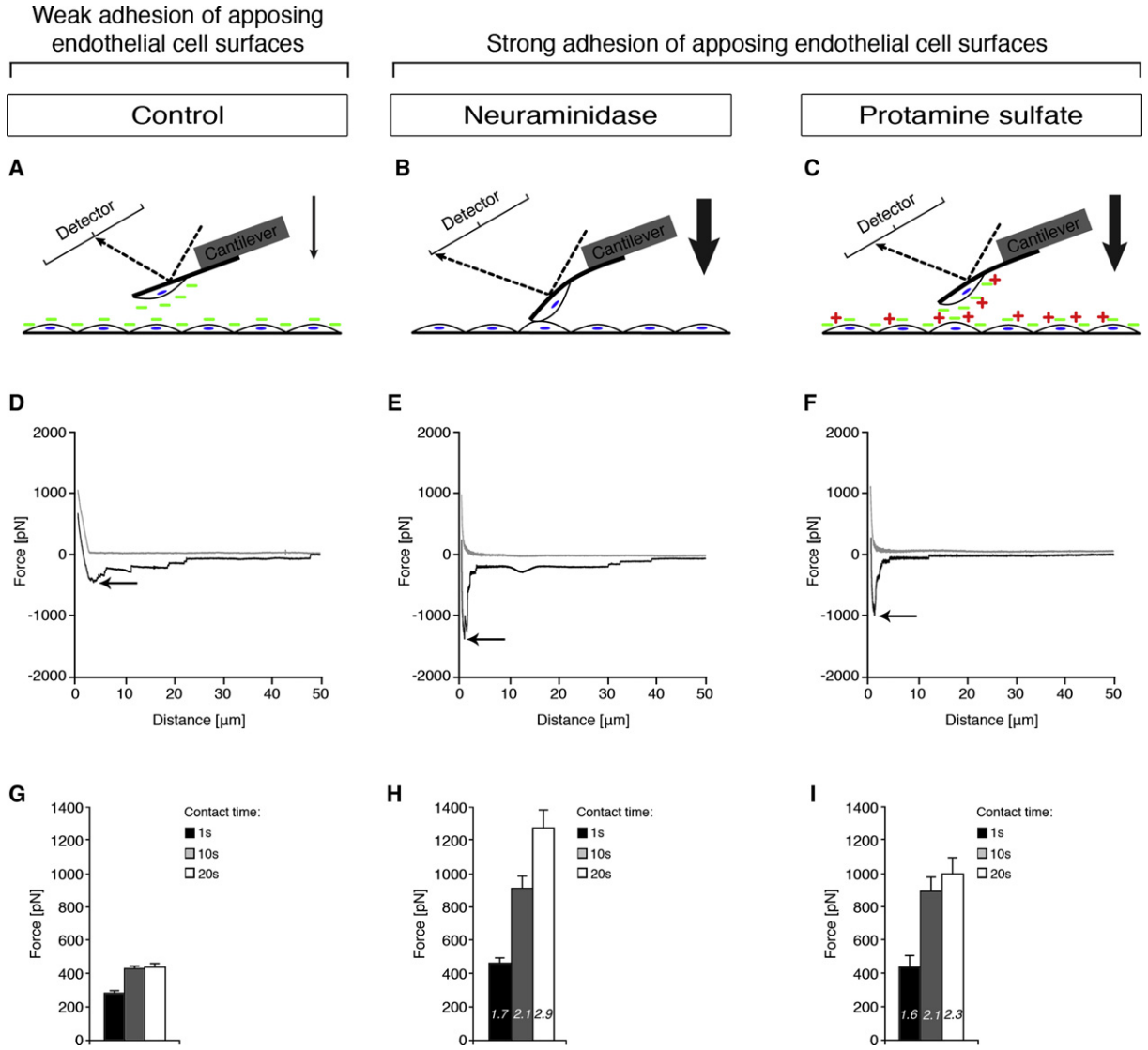

Figure 3. Quantification of Adhesion Forces between Apposing Endothelial Cell Surfaces after Neuraminidase and Protamine Sulfate Treatment by SCFS

(A–C) Schematic diagram of an adhesion experiment under (A) control conditions and after treatment with (B) neuraminidase or (C) protamine sulfate. The negative charges of sialic acids are shown in green (−) and the positive charges of protamine sulfate are shown in red (+). An EC grown onto an AFM cantilever was brought into contact with the EC monolayer. Black dashed lines indicate the laser beam to measure the cantilever deflection. After a given contact time (1 , 10 , or 20 s), the cantilever was withdrawn to separate the ECs and to measure their adhesive forces. Black arrows indicate the adhesive force between the single EC and the EC monolayer causing the cantilever to deflect downward. The thickness of the arrow reflects the magnitude of the adhesive strength between the cells.

(D–F) Representative force-distance curves (20 s) after treatment indicated above. Approach curves of the cantilevers toward the EC monolayer are shown in gray. Withdrawal curves are shown in black and are used to estimate the maximum adhesion force (arrow).

(G–I) Quantification of the adhesion force between ECs and an EC monolayer after 1 s (black bar), 10 s (gray bar), and 20 s (white bar) contact times and treatment indicated above. $n \geq 12$ independent experiments with $n \geq 56$ measurements per condition and contact time. All values are means ± SEM.

(H and I) Numbers on the bars indicate fold change compared to (G) control for the respective contact time.

force needed to separate them (Figures 3A–3C). Neuraminidase treatment increased endothelial cell-cell adhesion after a contact time of 1 s (1.7× increase, $p < 0.001$ compared to control), 10 s (2.1× increase, $p < 0.001$ compared to control), and 20 s (2.9× increase, $p < 0.001$ compared to control) (compare Figures 3A, 3D, and 3G with Figures 3B, 3E, and 3H). Moreover, the low adhesion force between apposing ECs could be restored by the addition of dextran sulfate but not by the addition of uncharged dextran (Figure S3). ECs treated with protamine sulfate also showed increasing cell-cell adhesion (1 s: 1.6× increase; 10 s: 2.1×; and 20 s: 2.3×; $p < 0.001$ compared to control) (compare Figures 3A, 3D, and 3G with Figures 3C, 3F, and 3I), but 30 min after washing, the low adhesion between ECs was restored at all contact times (data not shown). Thus, these force measurements directly confirm that ECs require the negative charge of sialic acids for lowering the cell-cell adhesion.

Lastly, we tested whether sialic acids and negative cell-surface charge were also required for lumen formation during sprouting angiogenesis (Figure 4), a process shown to be involved in blood vessel formation in the developing brain and retina as well as in the growing tumor [24–27]. Here, we

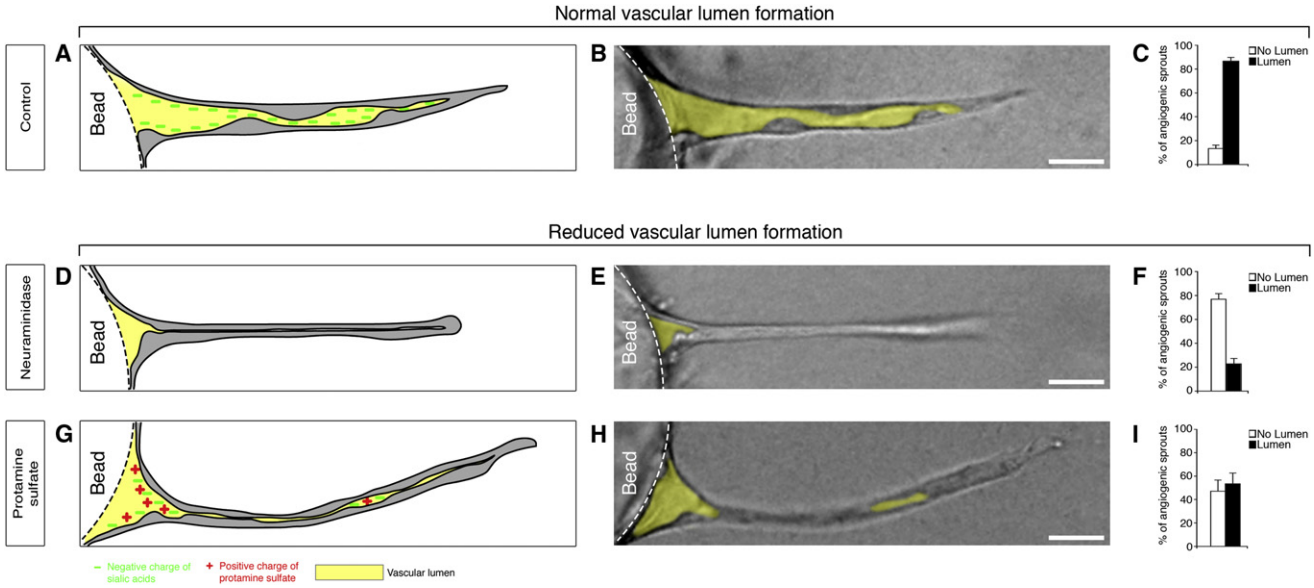

Figure 4. Sialic Acids and Negative Cell-Surface Charges Are Required for Vascular Lumen Formation In Angiogenic Sprouts

(A, D, and G) Schematic overviews on lumen formation in angiogenic sprouts under (A) control conditions and after treatment with (D) neuraminidase or (G) protamine sulfate. The negative charges of sialic acids are shown in green (−) and the positive charges of protamine sulfate are shown in red (+). The vascular lumen is indicated in yellow.

(B, E, H) Bright-field images of angiogenic sprouts 26 hr after the treatment indicated on the left. The vascular lumen is pseudocolored in yellow. See also Movie S3. Scale bars represent 20 μm.

(C, F, I) Quantification of lumen formation in sprouts 26 hr after the treatment indicated on the left. n ≥ 35 sprouts from n = 6 experiments per treatment. All values are means ± SEM.

employed an in vitro 3D sprouting angiogenesis assay [28], which reflects in vivo angiogenesis to a large extent [29–31]. We identified the vascular lumen in these sprouts based on bright-field and confocal light microscopic images. Using this assay, we found that sprouts harboring a small lumen developed into sprouts with virtually no vascular lumen upon neuraminidase treatment (compare Figures 4A–4C with Figures 4D–4F, and see Movie S3). Importantly, lumen formation was partially restored by the addition of dextran sulfate, but not by the addition of uncharged dextran (Figure S4). In addition, sprouts treated with protamine sulfate also showed a reduction in vascular lumen development (compare Figures 4A–4C with Figures 4G–4I, and see Movie S3). In both neuraminidase and protamine sulfate treatments, the apposing apical EC surfaces appear to adhere for longer times and thus have difficulties separating in order to form a continuous and growing vascular lumen (Movie S3). Therefore, the negative charge of sialic acids is also required for lumen formation in angiogenic sprouts in vitro.

Taken together, our findings show that the blood vessel lumen develops from the electrostatic repulsion of apposing EC surfaces. Because negatively charged glycoproteins, such as mucins and proteoglycans, are found on most luminal cell surfaces, such as the ones of tracheae, gut tubes, kidney tubules, pancreatic ducts, and the tubes of testis and mammary glands, it is possible that electrostatic repulsion is a general principle used to initiate lumen formation in many organs throughout the animal kingdom.

Experimental Procedures

Antibodies and Reagents

Goat anti-PODXL (R&D Systems), rat anti-PECAM-1 (BD Bioscience), rabbit anti-moesin (Abcam), Alexa Fluor 488 phalloidin (Invitrogen), and biotinylated *T. mobilensis* lectin [17] were used for immunostainings. DAPI (Sigma) was used to stain cell nuclei. Secondary antibodies were conjugated with AF488, AF633 (Molecular Probes), Cy3, or Cy5 (Jackson ImmunoResearch). Neuraminidase (0.5 U/ml, Sigma) or protamine sulfate (0.5 mg/ml, Sigma) was used for WEC, for BRA, and for SCFS experiments. Low-molecular-weight dextran (Sigma) and dextran sulfate (Sigma) were used at 1 mg/ml for WEC and at 10 mg/ml for BRA and SCFS. FITC conjugated dextran sulfate [32] was used at 1 mg/ml for labeling the neuraminidase-treated apical cell surfaces of aortic ECs. For the 3D sprouting angiogenesis assay, fibrinogen (2.5 mg/ml, Sigma), aprotinin (0.15 U/ml, Sigma), thrombin (4 U/ml, Sigma), neuraminidase (0.06 U/ml), dextran and dextran sulfate (0.05 mg/ml), and protamine sulfate (0.5 mg/ml) were used. Poly-DL-alanine (0.5 mg/ml, Sigma) or PBS served as controls in each assay.

Mouse Embryo Isolation, Embryonic Injections, and WEC

Isolated NMRI or CD1 mouse embryos (Janvier) were sorted by their numbers of somites. All embryos, after isolation or WEC, were fixed in 4% paraformaldehyde (PFA) in PBS and further processed for imaging. WEC was performed as previously described [1]. Briefly, all substances were injected into embryos at the 2S stage from the ventral side through the endoderm into the mesenchyme. After injection, embryos were roller-cultured for the indicated time periods and processed for immunostaining and imaging.

Immunostaining and Imaging

Immunostaining and imaging were performed as previously described [1]. Images were acquired and analyzed with a Zeiss Laser Scanning Microscope (LSM510 or LSM710) and ImageJ (National Institutes of Health, [NIH]), respectively. For the identification of ECs, all sections were costained for PECAM-1.

Cell Culture

HUVEC (Lonza) at a passage smaller than passage 6 were used for all experiments. HUVECs and human skin fibroblast cells (HSF Detroit 551, Promochem) were grown in EGM-2 medium (Lonza) and MEM (supplemented with 10% FCS), respectively, and incubated at 37°C and 5% CO_2. The media were changed every other day.

Bead Rolling Assay

HUVECs were seeded on collagen I-coated Cytodex-3 beads (GE Healthcare) and collagen I-coated wells of a 6-well plate. On the second day, ~100 HUVEC-coated beads were transferred to each well containing a confluent HUVEC monolayer, which was tilted by ~20 degrees. The rolling distance was subsequently recorded over 5 min (SMZ1500 and NIS-elements, Nikon) at 30 frames/min. Neuraminidase or protamine sulfate was subsequently added for 30 min, and the measurements were repeated. In addition, the cells were subsequently washed with fresh medium and incubated for 30 min or 24 hr, and rolling distances were then determined with the BRA. Alternatively, dextran or dextran sulfate was added for 30 min to neuraminidase-treated cells, and measurements were repeated. Rolling distances of the respective treatments were normalized to the controls and analyzed with ImageJ (NIH).

SCFS

SCFS experiments were conducted by using AFM as previously described [33]. In brief, HUVECs were cultured on a collagen I-coated coverslip. On the second day, the confluent coverslips were carefully rinsed with EGM-2 medium and built into a BioCell (JPK Instruments) for measurements at a physiological temperature (37°C) and JPK NanoWizard equipped with a CellHesion module (JPK Instruments) for long-distance pulling. Next, 50 μl of a single-cell suspension (~500 cells) was added into the BioCell, and a single cell was picked with a Concanavalin A-coated tipless AFM cantilever (NP-0, nominal spring constant 60 mN/m; Veeco Instruments) using a constant contact force of 1 nN. Adhesion measurements were carried out with an approach and retract velocity of 5 μm/s, a contact force of 1 nN, and a contact time randomly changed between 1, 10, and 20 s at different spots of the underlying monolayer. Force-distance curves were analyzed with custom procedures in IgorPro (Wavemetrics [23]). Before each experiment, spring constant measurements were performed on undecorated glass slides with the thermal noise method [34].

3D Sprouting Angiogenesis Assay

The 3D sprouting angiogenesis assay was performed as previously described [28]. Briefly, collagen I-coated Cytodex-3 beads were coated with HUVECs. On the next day, beads were resuspended in PBS containing fibrinogen and aprotinin and mixed with thrombin to yield a fibrin hydrogel. The solidified fibrin gel was subsequently overlaid with human skin fibroblasts (ATCC). PBS (control), neuraminidase, dextran, dextran sulfate, or protamine sulfate was added when a vascular lumen started to develop, and sprouts were imaged on an inverted microscope (Zeiss Axio Observer Z1) every 20 min for 26 hr. Per condition, six independent wells were imaged with five fields of view per well. Sprouts of a minimal length of 50 μm were counted at the end of the treatment period and classified as lumenized if more than 10% of the sprout length contained a visible lumen (measured from sprout stalk to sprout tip, starting at 20 μm distance from the bead). Sprout lumens were detected on the corresponding bright-field image as previously shown [31] and pseudocolored in yellow.

Statistical Analysis

Data are presented as mean ± standard deviation (SD) or ± standard error of the mean (SEM) (see figure legends). Student's t tests were used for statistical analyses. $p < 0.05$ was considered statistically significant.

Supplemental Information

Supplemental Information includes four figures and three movies and can be found with this article online at doi:10.1016/j.cub.2010.09.061.

Acknowledgments

We thank S. Jakob, R. Yu, D. Lingwood, F. Oesterhelt, and our friends and colleagues for their help. We are also grateful to R. Rieben and N. Bovin for their kind support and sharing the FITC-conjugated dextran sulfate. The German Research Foundation funded this project (DFG; LA1216/4-1).

Received: June 14, 2010
Revised: September 4, 2010
Accepted: September 24, 2010
Published online: October 21, 2010

References

1. Strilić, B., Kucera, T., Eglinger, J., Hughes, M.R., McNagny, K.M., Tsukita, S., Dejana, E., Ferrara, N., and Lammert, E. (2009). The molecular basis of vascular lumen formation in the developing mouse aorta. Dev. Cell *17*, 505–515.
2. Tarbell, J.M., and Ebong, E.E. (2008). The endothelial glycocalyx: A mechano-sensor and -transducer. Sci. Signal. *1*, pt8.
3. Ng, A.N., de Jong-Curtain, T.A., Mawdsley, D.J., White, S.J., Shin, J., Appel, B., Dong, P.D., Stainier, D.Y., and Heath, J.K. (2005). Formation of the digestive system in zebrafish: III. Intestinal epithelium morphogenesis. Dev. Biol. *286*, 114–135.
4. Kesavan, G., Sand, F.W., Greiner, T.U., Johansson, J.K., Kobberup, S., Wu, X., Brakebusch, C., and Semb, H. (2009). Cdc42-mediated tubulogenesis controls cell specification. Cell *139*, 791–801.
5. Braga, V.M., Pemberton, L.F., Duhig, T., and Gendler, S.J. (1992). Spatial and temporal expression of an epithelial mucin, Muc-1, during mouse development. Development *115*, 427–437.
6. Jones, S.J., and Baillie, D.L. (1995). Characterization of the let-653 gene in Caenorhabditis elegans. Mol. Gen. Genet. *248*, 719–726.
7. Dinglasan, R.R., Alaganan, A., Ghosh, A.K., Saito, A., van Kuppevelt, T.H., and Jacobs-Lorena, M. (2007). Plasmodium falciparum ookinetes require mosquito midgut chondroitin sulfate proteoglycans for cell invasion. Proc. Natl. Acad. Sci. USA *104*, 15882–15887.
8. Ayers, K.L., Gallet, A., Staccini-Lavenant, L., and Thérond, P.P. (2010). The long-range activity of Hedgehog is regulated in the apical extracellular space by the glypican Dally and the hydrolase Notum. Dev. Cell *18*, 605–620.
9. Tian, E., and Ten Hagen, K.G. (2007). A UDP-GalNAc:polypeptide N-acetylgalactosaminyltransferase is required for epithelial tube formation. J. Biol. Chem. *282*, 606–614.
10. Husain, N., Pellikka, M., Hong, H., Klimentova, T., Choe, K.M., Clandinin, T.R., and Tepass, U. (2006). The agrin/perlecan-related protein eyes shut is essential for epithelial lumen formation in the Drosophila retina. Dev. Cell *11*, 483–493.
11. Meder, D., Shevchenko, A., Simons, K., and Füllekrug, J. (2005). Gp135/podocalyxin and NHERF-2 participate in the formation of a preapical domain during polarization of MDCK cells. J. Cell Biol. *168*, 303–313.
12. Martin-Belmonte, F., Gassama, A., Datta, A., Yu, W., Rescher, U., Gerke, V., and Mostov, K. (2007). PTEN-mediated apical segregation of phosphoinositides controls epithelial morphogenesis through Cdc42. Cell *128*, 383–397.
13. Nielsen, J.S., and McNagny, K.M. (2008). Novel functions of the CD34 family. J. Cell Sci. *121*, 3683–3692.
14. Parker, L.H., Schmidt, M., Jin, S.W., Gray, A.M., Beis, D., Pham, T., Frantz, G., Palmieri, S., Hillan, K., Stainier, D.Y., et al. (2004). The endothelial-cell-derived secreted factor Egfl7 regulates vascular tube formation. Nature *428*, 754–758.
15. Blum, Y., Belting, H.G., Ellertsdottir, E., Herwig, L., Lüders, F., and Affolter, M. (2008). Complex cell rearrangements during intersegmental vessel sprouting and vessel fusion in the zebrafish embryo. Dev. Biol. *316*, 312–322.
16. Jin, S.W., Beis, D., Mitchell, T., Chen, J.N., and Stainier, D.Y. (2005). Cellular and molecular analyses of vascular tube and lumen formation in zebrafish. Development *132*, 5199–5209.
17. Babál, P., and Gardner, W.A., Jr. (1996). Histochemical localization of sialylated glycoconjugates with Tritrichomonas mobilensis lectin (TLM). Histol. Histopathol. *11*, 621–631.
18. Gelberg, H., Healy, L., Whiteley, H., Miller, L.A., and Vimr, E. (1996). In vivo enzymatic removal of alpha 2—>6-linked sialic acid from the glomerular filtration barrier results in podocyte charge alteration and glomerular injury. Lab. Invest. *74*, 907–920.
19. Eto, N., Kojima, I., Uesugi, N., Inagi, R., Miyata, T., Fujita, T., Johnson, R.J., Shankland, S.J., and Nangaku, M. (2005). Protection of endothelial cells by dextran sulfate in rats with thrombotic microangiopathy. J. Am. Soc. Nephrol. *16*, 2997–3005.
20. Laumonier, T., Mohacsi, P.J., Matozan, K.M., Banz, Y., Haeberli, A., Korchagina, E.Y., Bovin, N.V., Vanhove, B., and Rieben, R. (2004). Endothelial cell protection by dextran sulfate: A novel strategy to prevent acute vascular rejection in xenotransplantation. Am. J. Transplant. *4*, 181–187.
21. Takeda, T., McQuistan, T., Orlando, R.A., and Farquhar, M.G. (2001). Loss of glomerular foot processes is associated with uncoupling of podocalyxin from the actin cytoskeleton. J. Clin. Invest. *108*, 289–301.

22. Puech, P.H., Taubenberger, A., Ulrich, F., Krieg, M., Muller, D.J., and Heisenberg, C.P. (2005). Measuring cell adhesion forces of primary gastrulating cells from zebrafish using atomic force microscopy. J. Cell Sci. *118*, 4199–4206.
23. Krieg, M., Arboleda-Estudillo, Y., Puech, P.H., Käfer, J., Graner, F., Müller, D.J., and Heisenberg, C.P. (2008). Tensile forces govern germ-layer organization in zebrafish. Nat. Cell Biol. *10*, 429–436.
24. Tammela, T., Zarkada, G., Wallgard, E., Murtomäki, A., Suchting, S., Wirzenius, M., Waltari, M., Hellström, M., Schomber, T., Peltonen, R., et al. (2008). Blocking VEGFR-3 suppresses angiogenic sprouting and vascular network formation. Nature *454*, 656–660.
25. Gerhardt, H., Golding, M., Fruttiger, M., Ruhrberg, C., Lundkvist, A., Abramsson, A., Jeltsch, M., Mitchell, C., Alitalo, K., Shima, D., and Betsholtz, C. (2003). VEGF guides angiogenic sprouting utilizing endothelial tip cell filopodia. J. Cell Biol. *161*, 1163–1177.
26. Hellström, M., Phng, L.K., Hofmann, J.J., Wallgard, E., Coultas, L., Lindblom, P., Alva, J., Nilsson, A.K., Karlsson, L., Gaiano, N., et al. (2007). Dll4 signalling through Notch1 regulates formation of tip cells during angiogenesis. Nature *445*, 776–780.
27. Stenman, J.M., Rajagopal, J., Carroll, T.J., Ishibashi, M., McMahon, J., and McMahon, A.P. (2008). Canonical Wnt signaling regulates organ-specific assembly and differentiation of CNS vasculature. Science *322*, 1247–1250.
28. Nakatsu, M.N., Sainson, R.C., Aoto, J.N., Taylor, K.L., Aitkenhead, M., Pérez-del-Pulgar, S., Carpenter, P.M., and Hughes, C.C. (2003). Angiogenic sprouting and capillary lumen formation modeled by human umbilical vein endothelial cells (HUVEC) in fibrin gels: The role of fibroblasts and Angiopoietin-1. Microvasc. Res. *66*, 102–112.
29. Ridgway, J., Zhang, G., Wu, Y., Stawicki, S., Liang, W.C., Chanthery, Y., Kowalski, J., Watts, R.J., Callahan, C., Kasman, I., et al. (2006). Inhibition of Dll4 signalling inhibits tumour growth by deregulating angiogenesis. Nature *444*, 1083–1087.
30. Kleaveland, B., Zheng, X., Liu, J.J., Blum, Y., Tung, J.J., Zou, Z., Sweeney, S.M., Chen, M., Guo, L., Lu, M.M., et al. (2009). Regulation of cardiovascular development and integrity by the heart of glass-cerebral cavernous malformation protein pathway. Nat. Med. *15*, 169–176.
31. Nikolova, G., Strilic, B., and Lammert, E. (2007). The vascular niche and its basement membrane. Trends Cell Biol. *17*, 19–25.
32. Laumonier, T., Walpen, A.J., Maurus, C.F., Mohacsi, P.J., Matozan, K.M., Korchagina, E.Y., Bovin, N.V., Vanhove, B., Seebach, J.D., and Rieben, R. (2003). Dextran sulfate acts as an endothelial cell protectant and inhibits human complement and natural killer cell-mediated cytotoxicity against porcine cells. Transplantation *76*, 838–843.
33. Puech, P.H., Poole, K., Knebel, D., and Muller, D.J. (2006). A new technical approach to quantify cell-cell adhesion forces by AFM. Ultramicroscopy *106*, 637–644.
34. Hutter, J.L., and Bechhoefer, J. (1993). Calibration of atomic-force microscope tips. Rev. Sci. Instrum. *64*, 1868–1873.